SHRP-S/FR-90-002

# Electrochemical Chloride Removal and Protection of Concrete Bridge Components (Injection of Synergistic Corrosion Inhibitors)

Marianna F. Asaro
Ann T. Gaynor
Samson Hettiarachchi

SRI International
333 Ravenswood Avenue
Menlo Park, California

**Strategic Highway Research Program**
National Research Council
Washington, D.C. 1990

SHRP-S/FR-90-002
Contract C-102C

October 1990

Strategic Highway Research Program
2101 Constitution Avenue, N.W.
Washington, D.C. 20418

(202) 334-3774

# REPORT DOCUMENTATION PAGE

*Form Approved*
*OMB No. 0704-0188*

PB91-122515

**2. REPORT DATE**
OCTOBER 1990

**3. REPORT TYPE AND DATES COVERED**
Final report

**4. TITLE AND SUBTITLE**
Electrochemical Chloride Removal and Protection of Concrete Bridge Components (Injection of Corrosion Inhibitors)

**5. FUNDING NUMBERS**
C-102C

**6. AUTHOR(S)**
Marianna F. Asaro, Ann T. Gaynor, Samson Hettiarachchi

**7. PERFORMING ORGANIZATION NAME(S) AND ADDRESS(ES)**
SRI International
333 Ravenswood Avenue
Menlo Park CA 94025

**8. PERFORMING ORGANIZATION REPORT NUMBER**
SHRP-S/FR-90-002

**9. SPONSORING/MONITORING AGENCY NAME(S) AND ADDRESS(ES)**
Strategic Highway Research Program
Suite 400
818 Connecticut Avenue N.W.
Washington, D.C. 20006

**10. SPONSORING/MONITORING AGENCY REPORT NUMBER**
SHRP/S/FR-90/002

**11. SUPPLEMENTARY NOTES**
SRI International is a subcontractor of Eltech Research Corp.

**12a. DISTRIBUTION/AVAILABILITY STATEMENT**
Available to the general public from NTIS and from the Transportation Research Board, National Academy of Sciences, 2101 Constitution Avenue N.W.
Washington, D.C. 20418; (202) 324-3250.

**12b. DISTRIBUTION CODE**
None

**13. ABSTRACT** *(Maximum 200 words)*

This final report states the findings of SRI International's feasibility study on the injection of synergistic corrosion inhibitors for the protection of concrete bridge components. Corrosion inhibitors were developed that can be electrically injected into concrete matrices using an in situ technique. The study showed that such inhibitor injection can provide adequate corrosion protection to rebars embedded in chloride-contaminated concrete. It was demonstrated that inhibitors developed under this project provide 78 to 85 percent corrosion protection for the rebars.

An important advantage of this technique is that the equipment required is similar to that used in cathodic protection, and therefore it is familiar to highway engineers. Another advantage is that inhibitor injection requires a temporary installation for only a few days, whereas cathodic protection requires a permanent installation.

**14. SUBJECT TERMS**
electrochemical chloride removal, concrete, chloride removal, corrosion inhibitors, rebar, cathodic protection

**15. NUMBER OF PAGES**
53

**16. PRICE CODE**

| **17. SECURITY CLASSIFICATION OF REPORT** | **18. SECURITY CLASSIFICATION OF THIS PAGE** | **19. SECURITY CLASSIFICATION OF ABSTRACT** | **20. LIMITATION OF ABSTRACT** |
|---|---|---|---|
| Unclassified | Unclassified | Unclassified | UL |

# GENERAL INSTRUCTIONS FOR COMPLETING SF 298

The Report Documentation Page (RDP) is used in announcing and cataloging reports. It is important that this information be consistent with the rest of the report, particularly the cover and title page. Instructions for filling in each block of the form follow. It is important to ***stay within the lines*** to meet ***optical scanning requirements***.

**Block 1**. Agency Use Only *(Leave blank)*.

**Block 2.** Report Date. Full publication date including day, month, and year, if available (e.g. 1 Jan 88). Must cite at least the year.

**Block 3.** Type of Report and Dates Covered. State whether report is interim, final, etc. If applicable, enter inclusive report dates (e.g. 10 Jun 87 - 30 Jun 88).

**Block 4.** Title and Subtitle. A title is taken from the part of the report that provides the most meaningful and complete information. When a report is prepared in more than one volume, repeat the primary title, add volume number, and include subtitle for the specific volume. On classified documents enter the title classification in parentheses.

**Block 5.** Funding Numbers. To include contract and grant numbers; may include program element number(s), project number(s), task number(s), and work unit number(s). Use the following labels:

| | | | |
|---|---|---|---|
| **C** | Contract | **PR** | Project |
| **G** | Grant | **TA** | Task |
| **PE** | Program Element | **WU** | Work Unit Accession No. |

**Block 6.** Author(s). Name(s) of person(s) responsible for writing the report, performing the research, or credited with the content of the report. If editor or compiler, this should follow the name(s).

**Block 7.** Performing Organization Name(s) and Address(es). Self-explanatory.

**Block 8.** Performing Organization Report Number. Enter the unique alphanumeric report number(s) assigned by the organization performing the report.

**Block 9.** Sponsoring/Monitoring Agency Name(s) and Address(es). Self-explanatory.

**Block 10.** Sponsoring/Monitoring Agency Report Number. *(If known)*

**Block 11.** Supplementary Notes. Enter information not included elsewhere such as: Prepared in cooperation with...; Trans. of...; To be published in.... When a report is revised, include a statement whether the new report supersedes or supplements the older report.

**Block 12a.** Distribution/Availability Statement. Denotes public availability or limitations. Cite any availability to the public. Enter additional limitations or special markings in all capitals (e.g. NOFORN, REL, ITAR).

**DOD** - See DoDD 5230.24, "Distribution Statements on Technical Documents."
**DOE** - See authorities.
**NASA** - See Handbook NHB 2200.2.
**NTIS** - Leave blank.

**Block 12b.** Distribution Code.

**DOD** - Leave blank.
**DOE** - Enter DOE distribution categories from the Standard Distribution for Unclassified Scientific and Technical Reports.
**NASA** - Leave blank.
**NTIS** - Leave blank.

**Block 13.** Abstract. Include a brief *(Maximum 200 words)* factual summary of the most significant information contained in the report.

**Block 14.** Subject Terms. Keywords or phrases identifying major subjects in the report.

**Block 15.** Number of Pages. Enter the total number of pages.

**Block 16.** Price Code. Enter appropriate price code *(NTIS only)*.

**Blocks 17. - 19.** Security Classifications. Self-explanatory. Enter U.S. Security Classification in accordance with U.S. Security Regulations (i.e., UNCLASSIFIED). If form contains classified information, stamp classification on the top and bottom of the page.

**Block 20.** Limitation of Abstract. This block must be completed to assign a limitation to the abstract. Enter either UL (unlimited) or SAR (same as report). An entry in this block is necessary if the abstract is to be limited. If blank, the abstract is assumed to be unlimited.

# Contents

Acknowledgments . . . . . . . . . . . . . . . . . . . . . . . . . . . . . . . . . . . . . . . . . . . . i

Abstract . . . . . . . . . . . . . . . . . . . . . . . . . . . . . . . . . . . . . . . . . . . . . . . . . 1

Executive Summary . . . . . . . . . . . . . . . . . . . . . . . . . . . . . . . . . . . . . . . . . . 3

Introduction . . . . . . . . . . . . . . . . . . . . . . . . . . . . . . . . . . . . . . . . . . . . . . . 5

Experimental Details . . . . . . . . . . . . . . . . . . . . . . . . . . . . . . . . . . . . . . . . . 9
  Selection and Synthesis of Inhibitor Compounds . . . . . . . . . . . . . . . . . . 9
  Experimental Solution and Sample Preparation . . . . . . . . . . . . . . . . . . . 10
  Evaluation of Corrosion Inhibition Effectiveness . . . . . . . . . . . . . . . . . . 10
    Theoretical Basis of Measurements . . . . . . . . . . . . . . . . . . . . . . . 10
    AC Impedance Method . . . . . . . . . . . . . . . . . . . . . . . . . . . . . . . . 11
    Evaluation of Corrosion Inhibitor Efficiency . . . . . . . . . . . . . . . . . 11
    Transport Number of Inhibitor Cation . . . . . . . . . . . . . . . . . . . . . 12
    Construction of Cell . . . . . . . . . . . . . . . . . . . . . . . . . . . . . . . . . 12
    Selection of Electrolyte and Inhibitors . . . . . . . . . . . . . . . . . . . . . 12
    Preparation of Concrete Disks and Columns . . . . . . . . . . . . . . . . . 14

Electromigration Studies . . . . . . . . . . . . . . . . . . . . . . . . . . . . . . . . . . . . . 15
  Analysis of Solution Following Electromigration . . . . . . . . . . . . . . . . . . 15
  Analysis of Disk Samples for Presence of Ionic Species
    Following Electromigration . . . . . . . . . . . . . . . . . . . . . . . . . . . . . 16

Inhibitor Injection Studies . . . . . . . . . . . . . . . . . . . . . . . . . . . . . . . . . . . . 17

Results and Discussion . . . . . . . . . . . . . . . . . . . . . . . . . . . . . . . . . . . . . . . 21
    Quaternary Ammonium Inhibitors . . . . . . . . . . . . . . . . . . . . . . . . . . . . . 21
    Quaternary Phosphonium Inhibitors . . . . . . . . . . . . . . . . . . . . . . . . . . . 21
    Optimization of Inhibitor Cation Injection . . . . . . . . . . . . . . . . . . . . . . . 26
    Transport Numbers of TBP+ Cation . . . . . . . . . . . . . . . . . . . . . . . . . . . 26
    Transport Numbers of TEP+ Cation . . . . . . . . . . . . . . . . . . . . . . . . . . . 28
    Electrical Injection of TBP+ and TEP+ Cations (as 100mM Solution . . . . . . . . . . . . . . . . . . . . . . . . . . . . . . . . . . . . . . 30
    Inhibitor Injection into Mortar Matrices . . . . . . . . . . . . . . . . . . . . . . . . 33
    Inhibitor Injection into Concrete Matrices . . . . . . . . . . . . . . . . . . . . . . . 33
    Transport Numbers of TEP+ Cation Through Concrete Matrices . . . . . . . . . 36
    Effectiveness of $TEPNO_2$ as a Corrosion Inhibitor for Rebar Steel Embedded in Concrete . . . . . . . . . . . . . . . . . . . . . . . . . . . . 37
    Inhibitor Injection into Mortar and Concrete Columns . . . . . . . . . . . . . . . . 39
    Injection of Corrosion Inhibitors into Concrete Blocks . . . . . . . . . . . . . . . . 41

Accomplishments and Conclusions . . . . . . . . . . . . . . . . . . . . . . . . . . . . . 47

Recommendations . . . . . . . . . . . . . . . . . . . . . . . . . . . . . . . . . . . . . . . 51

References . . . . . . . . . . . . . . . . . . . . . . . . . . . . . . . . . . . . . . . . . . 53

# Acknowledgments

The research described herein was supported by the Strategic Highway Research Program (SHRP). SHRP is a unit of the National Research Council that was authorized by section 128 of the Surface Transportation and Uniform Relocation Assistance Act of 1987.

# Abstract

SRI International undertook this feasibility study on the injection of synergistic corrosion inhibitors for protection of concrete bridge components for the Strategic Highway Research Program (SHRP) under contract SHRP 87-C-102C. During this study, SRI developed corrosion inhibitors that can be electrically injected into concrete matrices using an *in situ* technique. SRI showed that such inhibitor injection can provide adequate corrosion protection to rebars embedded in chloride-contaminated concrete. It was demonstrated that inhibitors developed under this project provide 78-85% corrosion protection for the rebars. Important advantages of this technology are its novelty and nondestructive nature, and the requirement of only temporary installation.

SRI believes that this technology can be improved further to provide 90-100% corrosion protection for rebar steel. The electrical field and the current density requirements are 5-10 V/cm and 0.46-1.24 mA/cm$^2$ (0.4-1.1 A/sq. ft.) respectively. The inhibitor injection rate increases 3-4 times when the current density is doubled. The current densities required for inhibitor injection are approximately 1,000 times higher than those used for cathodic protection, and 2-5 times lower than those used for electrochemical chloride removal.

# Executive Summary

SRI International performed this feasibility study on the injection of synergistic corrosion inhibitors for protection of concrete bridge components for the Strategic Highway Research Program (SHRP) under contract SHRP 87-C-102C. During this research, SRI developed electrically injectable corrosion inhibitors that provide 78-85% corrosion protection for the rebars. This technology can be further improved to provide 90-100% corrosion protection for rebar steel. Inhibitor injection requires approximately 1,000 times higher current densities than those used for cathodic protection.

An important advantage of this technique is that the equipment required is similar to that used in cathodic protection, and hence, is familiar to highway bridge engineers. However, unlike cathodic protection, which requires a permanent installation, protection using inhibitor injection requires only a temporary installation for a few days.

Based on the experiment results, the following conclusions can be made on the electrical injection of corrosion inhibitors.

- Effective inhibitor injection occurs at an electrical field of 5 to 10 V/cm at a current density of 0.46 to 1.24 mA/cm$^2$ (0.4-1.1 A/sq. ft.) within a period of 10 to 15 days.

- At current densities of 0.50, 1.00, and 2-3 mA/cm$^2$, the inhibitors' injection rate increased in the order 35, 95, and 420 $\mu$g/cm$^2$/hr. respectively for TEPNO$_2$. Thus, a doubling of the current density provides an approximate 3 to 4 time increase in the inhibitor injection rate. In a practical sense, a current density of approximately 1 mA/cm$^2$ appears desirable.

- An inhibitor injection current density of 1 $mA/cm^2$ (900 $mA/ft^2$) is 900 times higher than that required for cathodic protection (i.e., 1 $mA/ft^2$). Thus, under rebar cathodic control, the inhibitor injection rate could be more than 1,000 times slower, requiring longer times to achieve the desired corrosion protection.

- After inhibitor injection, the rebar potential continues to shift in the positive direction over the tested period of 3 to 4 weeks, indicating that chloride remigration, if it does occur, is not effective in increasing the rebar corrosion rate. However, a long-term study ($>12$ months) with sodium chloride ponding is necessary before a decision is made on the effectiveness of the inhibitor injection chloride remigration.

# 1

# Introduction

SRI International undertook this feasibility study on the injection of synergistic corrosion inhibitors for protection of concrete bridge components for the Strategic Highway Research Program (SHRP) under Contract No. SHRP-87-C102C. We explored the use of our unique synergistic corrosion inhibitor technology to protect chloride-contaminated steel rebars from corrosion. Our inhibitors become more efficient as the chloride concentration increases, thereby automatically compensating for chloride remigration. The inhibitors are cationic, i.e., positively charged, and hence can be applied to bridge decks with chloride removal, simultaneously substantially reducing the complexity of the protection system.

We completed the synthesis and evaluation of quaternary ammonium and phosphonium corrosion inhibitors. The anions used with these inhibitors include chloride, nitrite, and molybdate ions. We studied the influence of the size and type of quaternary cation and the type of the supporting anion on the corrosion inhibition efficiency of steel in 5% NaCl solution having a pH of 10-10.5. We also synthesized and evaluated the molybdate analogs of the quaternary compounds with the desirable anions by starting from their chloride or bromide analogs and performing an ion-exchange process to obtain the nitrites and the molybdates.

After synthesizing the corrosion inhibitors, we performed preliminary studies of electrical injection of inhibitors into cement paste disks. The anionic inhibitors included nitrite and molybdate ions, while the cationic inhibitor was primarily tetraethylphosphonium ion ($TEP^+$). The counter anion was chloride, nitrite, or molybdate ion. Initially, electromigration experiments were performed with the inhibitor dissolved in 5% NaCl solution having a pH of 10.5. Because of excessive chlorine gas evolution at the anode, we changed the solution to 0.285 M $Na_2SO_4$, which had the same ionic strength as the 5% NaCl solution. This solution was replaced subsequently by a saturated solution of calcium hydroxide to simulate the practical environmental conditions present in concrete.

The experiments were performed in a two-compartment cell whose compartments were separated by a 1-cm-thick mortar or concrete disk. Both compartments were filled with electrolyte solution, i.e., 5% NaCl, 0.285 M $Na_2SO_4$, or saturated $Ca(OH)_2$. In the cationic inhibitor injection studies, the inhibiting ion was added to the anode compartment. The extent of inhibitor injection was determined by analyzing for a predetermined time the originally inhibitor-free compartment for the presence of the inhibitor ion after application of an electrical field. The presence of the inhibitor in the mortar or concrete was confirmed by crushing a sample of the matrix,extracting it with boiling water, and analyzing the resulting solution for the inhibitor ion. Analysis of all ionic species was done with ion-chromatography. Electrodes used in the electromigration studies were primarily dimensionally stable anodes (DSA$^{TM}$) supplied by ELTECH Research Corporation.

During the optimization studies we showed that an electrical field of 5 V/cm is sufficient to obtain sufficient mobility of inhibitor cations through the cured mortar matrices. We proved that the inhibitor cation movement is electrical field-assisted, by conducting a simple diffusion experiment without an applied electrical field. This experiment showed no movement of the inhibitor cations to the cathode compartment of the cell even after 19 days of testing. We also showed that ionic movement through cured disks is slower than that through uncured disks.

We determined the polarization resistance ($R_p$) of rebar steel samples embedded in 8-in. high cured mortar columns at depths of 2 and 7 in. from the top of the column. The mortar in the columns had a cement:sand:water composition of 1:3:0.5 and contained 15 lb/yd$^3$ of $Cl^-$ ions.

We also determined the transport number of inhibitor cations through concrete matrices. In these studies, we used 2-cm-thick concrete disks. The transport numbers of $TEP^+$ cations were determined at electrical fields of 5, 10, and 20 V/cm over an electrical injection period of 10-12 days. The concrete had a cement:sand:aggregate:water composition of 1:2.2:2.75:0.5 and contained 15 lb/yd$^3$ of $Cl^-$ ions. The corrosion potential ($E_{corr}$) variation of the rebar steel was also monitored during the inhibitor injection period.

As the inhibitor was being injected, AC impedance measurements of the embedded steel samples were also made to determine the $R_p$ of the steel and hence to obtain a general idea of the corrosion rate and its variation.

A study was also undertaken in which tetraethylphosphonium nitrite ($TEPNO_2$) and a known inhibitor formulation were mixed into concrete. The corrosion rate of the steel in these mixtures was compared to that of a steel sample embedded in concrete free of any inhibitors. The results showed that $TEPNO_2$ developed during this project is comparable to a patented commercial inhibitor formulation.

To improve and enhance the corrosion protection afforded to rebar steel by $TEPNO_2$, we studied concrete blocks with new and different inhibitor formulations containing $TEPNO_2$ applied under electrical injection conditions. These studies showed that the $E_{corr}$ of rebar steel embedded in chloride-contaminated concrete increases in the positive direction and reaches 78-85% protection levels after the inhibitor has been injected over a period of 5-10 days.

Based on the experimental results, following conclusions were made concerning the anticipated research results of the electrical injection of corrosion inhibitors.

- Effective inhibitor injection occurs at an electrical field of 5 to 10 V/cm at a current density of 0.46 to 1.24 $mA/cm^2$ (0.4 - 1.1 A/sq. ft.) within a period of 10-15 days.

- At current densities of 0.50, 1.00 and 2-3 $mA/cm^2$ the inhibitor injection rate increased in the order 35, 95 and 420 $\mu g/cm^2/hr$ respectively for $TEPNO_2$. Thus, a doubling of the current density provides an approximately 3 to 4 times increase in the inhibitor injection rate. In a practical sense, a current density of approximately 1 $mA/cm^2$ appears desirable.

- An inhibitor injection current density of 1 $mA/cm^2$ (900 $mA/ft^2$) is 900 times higher than that required for cathodic protection (i.e. 1 $mA/ft^2$). Thus, under rebar cathodic control, the inhibitor injection rate could be more than 1000 times slower, requiring longer times to achieve the desired corrosion protection.

- After inhibitor injection, the rebar potential continues to shift in the positive direction over the tested period of 3 to 4 weeks indicating that chloride remigration, if it does occur, is not effective in increasing the rebar corrosion rate. However, a long term study (> 12 months) with sodium chloride ponding is necessary before a decision is made on the effectiveness of the inhibitor injection against chloride remigration.

It is critically important to determine how long the inhibitor remains effective before this technology is field tested. During the feasibility study conducted, it appears that the inhibitor remains effective over the longest period tested i.e. approximately one month. Thus, a long term study lasting one to two years will be necessary to determine the long term effectiveness of the inhibitor. It is important to note that in a future study, the inhibitor effectiveness might be further improved to achieve corrosion protection levels greater than 90%.

Experiments with $TEPNO_2$ show that an inhibitor content of approximately 5 to 20 $mg/cm^2$ of the concrete surface provides adequate protection to the rebar. If the inhibitor effectiveness is further improved in a future study, the required inhibitor content can be drastically reduced. Thus, it is important to perform a study with improved inhibitor formulations.

The current cost of chemical synthesis is considerably higher than the arbitrary cost of $15/sq. ft. estimated by SHRP. It is unrealistic to perform cost calculations based on small samples of chemicals purchased from chemical suppliers during this project. When a barrel of a chemical is purchased, the cost involved is much lower than when a 5 g quantity is purchased. Besides, as the demand increases chemicals can be synthesized in bulk quantities resulting in cost reduction. The labor costs could be reduced by almost 1000 fold during bulk production compared with synthesis performed in a research laboratory. Furthermore, cost estimates must be prepared once the inhibitor is optimized. If the inhibitor is more effective, then the quantity required for corrosion protection is lower, resulting in cost reduction. SRI believes that it is too early to make a realistic prediction of the inhibitor costs involved in the light of the above facts. However, the overall cost of this technology could be much lower than that required for cathodic protection because inhibitor injection is less labor intensive, does not require a permanent installation and can be practiced in-situ.

# 2

# Experimental Details

## Selection and Synthesis of Inhibitor Compounds

We studied a variety of commercially available quaternary ammonium and phosphonium compounds having the general structures

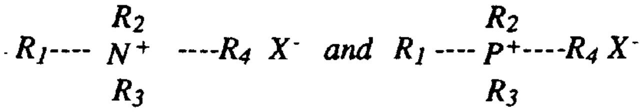

$$R_1\text{----}\underset{R_3}{\overset{R_2}{N^+}}\text{----}R_4\ X^- \quad \text{and} \quad R_1\text{----}\underset{R_3}{\overset{R_2}{P^+}}\text{----}R_4\ X^-$$

in which $R_1$, $R_2$, $R_3$, and $R_4$ are alkyl or aryl groups and $X^-$ is a halide ion. The substituents $R_1$ through $R_4$ were selected to vary the size, hydrophobicity, aromaticity, and charge stabilization of the inhibitor molecules.

Quaternary ammonium nitrites and molybdates were formed by replacing the halide ion with the nitrite, or the molybdate ion by means of ion exchange. The ion exchange was accomplished by mixing 10 g of the ion-exchange resin (Amberlite IRA-400) with 1 L of solution containing 2.3 g sodium nitrite or 8.1 g sodium molybdate and stirring the resulting suspension for 24 hours. The solution was then filtered to obtain the ion-exchange resin containing the nitrite or the molybdate ion. One gram of the ion-exchange resin was subsequently mixed with 100 mL of a 10 mM aqueous solution of the quaternary ammonium (or phosphonium) halide and stirred for 20-24 hours to exchange the halide of the quaternary salt with the nitrite or molybdate ion in the resin. Ion exchange appears to occur readily with the salts tested.

## Experimental Solution and Sample Preparation

All corrosion inhibitor screening studies were performed with rotating cylinder electrodes made of the rebar steel used in concreting applications. The rotation arrangement provides better hydrodynamics and renders much higher mass transfer rates at reasonably slow rotational speeds. The area of each electrode was 1 $cm^2$, and the speed of rotation was kept constant at 500 rpm. Each electrode was polished with 600-grit emery paper, then degreased with methanol and rinsed with water before introduction into the cell. We used a 5% NaCl aqueous solution whose pH was adjusted to 10.5 by the dropwise addition of 1 M NaOH. The quaternary inhibitor concentration was 10 mM in most screening studies.

## Evaluation of Corrosion Inhibitor Effectiveness

The inhibitors were rapidly screened by AC impedance spectroscopy. The theoretical basis of these measurements is discussed below, and details of the method are then described in the following pages.

## Theoretical Basis of Measurements

The polarization resistance ($R_p$) of a corroding system under activation control is defined as

$$R_p = \left(\frac{\partial E}{\partial I}\right)_{E = E_{corr}} \tag{2.1}$$

Once the $R_p$ is known, the corrosion rate of the metal can be evaluated by using the Stern-Geary relationship (1). Thus,

$$I_{corr} = \frac{b_a b_c}{2.303(b_a + b_c)} \frac{1}{R_p} \tag{2.2}$$

where $I_{corr}$ is the corrosion current and $b_a$ and $b_c$ are the anodic and cathodic Tafel slopes, respectively. In these studies, however, an exact evaluation of $I_{corr}$ is not required because $I_{corr}$ is inversely proportional to $R_p$, and $b_a$ and $b_c$ are assumed to be constants for a particular metal in a given environment. Thus,

$$I_{corr} = \frac{K}{R_p} \tag{2.3}$$

where

$$K = \frac{b_a b_c}{2.303(b_a + b_c)} \qquad (2.4)$$

The advantage of this method is that $R_p$ measurements can be performed with minimum system perturbation by using AC impedance spectroscopy.

Great care must be taken when using equation (2.3) for corrosion rate measurements because the K value need not remain constant whether or not the inhibitor is present. It may even vary from one inhibitor to another because different inhibitors may result in different anodic and cathodic Tafel slopes ($b_a$ and $b_c$). These slopes are likely to be different because $b_a$ and $b_c$ are system-dependent parameters.

## AC Impedance Method

AC impedance measurements were performed at the free corrosion potential by holding the potential at this value with a PAR Model 273 potentiostat. The interfacial impedance was measured over a wide frequency range (1 kHz to 30 mHz or less, depending on the system studied) using a Solartron Model 1250 transfer function analyzer. The wideband AC impedance measurements, which provide information on both the resistive and the capacitive behavior of the interface, make it possible to evaluate the corrosion behavior of an inhibitor-coated metal. In this analysis, the high-frequency intercept of the real axis impedance gives the solution resistance ($R_s$), whereas the low-frequency intercept gives a summation of both $R_s$ and $R_p$. Once $R_p$ is known, the corrosion rate of the metal can be evaluated using equation (2.2).

AC impedance spectra also provide information on the impedance of the inhibitor layer, the development over time of active sites such as pores in the inhibitor layer, the adsorption capacitance arising from the presence of the inhibitor, and the presence or absence of diffusional processes and potential-dependent surface relaxation processes associated with coverage by the inhibiting species at lower frequencies and by the anodic intermediate species at higher frequencies.(2,3) Thus, high-frequency data provide information on the inhibitor coating characteristics governed by the adsorption capacitance, whereas low-frequency data provide information on Faradaic and surface relaxation processes associated with inhibitor adsorption.

## Evaluation of Corrosion Inhibitor Efficiency

Corrosion inhibitor efficiency (*IE*) is defined as

$$IE = \frac{I^{o}_{corr} - I^{I}_{corr}}{I^{o}_{corr}} \times 100 \qquad (2.5)$$

where $I^{o}_{corr}$ and $I^{I}_{corr}$ are the corrosion currents of the metal in the absence and presence of the inhibitor, respectively. From equations (2.3) and (2.5), we obtain

$$IE = \frac{R_P^I - R_P^o}{R_P^I} x\ 100 \tag{2.6}$$

where $R_p^I$ and $R_p^o$ are the polarization resistances with and without the inhibitor, respectively assuming K in eq. (2.3) to be a constant. The IE measurement using equation (2.6) can be performed with either the polarization resistance technique or the AC impedance technique.

## Transport Numbers of Inhibitor Cations

Transport number is defined as the fraction of the total current carried by a charged species. Estimation of the transport numbers of inhibitor cations and the electromigration studies were performed in a two-compartment cell. The cell was designed so that a 2-cm-thick mortar or concrete disk could be sandwiched between the two compartments. The electrolyte was a solution of saturated $Ca(OH)_2$. The inhibitor was $TEPNO_2$ at a concentration of 100 mM. Electrical fields of 5, 10, and 20 V/cm were used in the inhibitor cation transport studies.

## Construction of Cell

We constructed a two-compartment glass cell that could have a concrete or mortar disk sandwiched between the two compartments (Figure 2-1). Liquid leakage between the glass rim and the concrete disk was avoided by either placing two O-rings or epoxying rubber gaskets on both sides of the disk. The two compartments and the concrete disk were kept in place by a clamp mounted with nuts and bolts as shown in Figure 2-1.

## Selection of Electrolyte and Inhibitors

A few experiments were performed with a solution of 5% NaCl at a pH of 10.5, which was subsequently replaced by a 0.285 M $Na_2SO_4$ solution at pH 10.5 with the same ionic strength. The reason for this replacement was the excessive chlorine gas evolution observed at the anode when NaCl was used as the electrolyte. A few experiments were performed with saturated $Ca(OH)_2$, an electrolyte that closely represents the practical environmental conditions present in concrete.

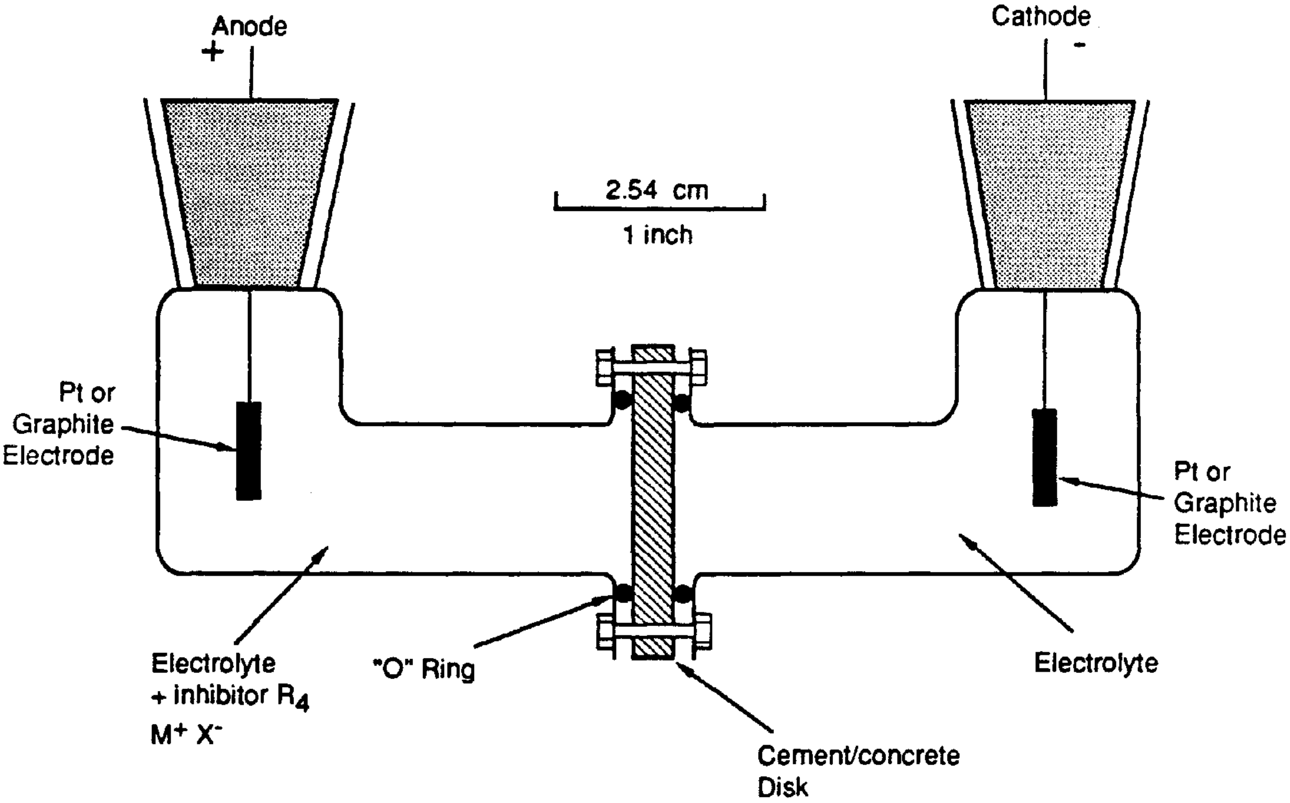

Figure 2-1. A schematic diagram of the cell used for electromigration studies of inhibitor cations through cement/concrete.

The synergistic inhibitors used were primarily tetraethyl- and tetrabutylphosphonium molybdate and nitrite at a concentrations of 10 and 100 mM.

## Preparation of Concrete Disks and Columns

Concrete disks and columns had a cement:sand:aggregate:water composition of 1:2.2:2.75:0.5. This formulation of concrete is equivalent to 612 lb/yd$^3$ of cement, 1310 lb/yd$^3$ of sand, 1662 lb/yd$^3$ of aggregate, and 306 lb/yd$^3$ of water, which is typical of a concrete composition with a mixture of coarse and fine aggregates. The concrete formulation also included 15 lb/yd$^3$ of $Cl^-$ added as NaCl. Both concrete disks and columns were cured before testing for 28 days in a humid plastic bag. Cement disks, used for comparison, had a cement:sand:water composition of 1:3:0.5 and a cross-sectional area of 7.1 cm$^2$.

# 3

# Electromigration Studies

Electromigration experiments were performed using the cell shown in Figure 2-1 with a mortar or concrete disk sandwiched between the two glass compartments. The electrolyte used was 5% NaCl, 0.285 M $Na_2SO_4$, or saturated $Ca(OH)_2$. When tetrabutylphosphonium molybdate or nitrite was used, the cationic inhibitor was introduced into the anode (positive) compartment. Once the disk, the electrolyte, and the inhibitor were in place in the cell, voltage was applied across the disk through DSA electrodes immersed in the solutions of the two compartments. Typical voltage applied across the cell varied from 10 to 40 V DC, and current varied from 10 to 40 mA depending on the number of cells connected in parallel. After the voltage was applied for a predetermined period of time, samples were collected from the two compartments of the cell for analysis of ionic species by ion-chromatography. The transport numbers of cations and anions were estimated from the concentration changes in the anolyte and catholyte caused by electrical field application. Variables studied during electrical injection of inhibitors included the applied DC voltage, duration of electromigration, and concentration of inhibitor.

## Analysis of Solutions Following Electromigration

Analysis of the ionic species present in anodic and cathodic compartments after electromigration tests was performed by ion-chromatography. An advantage of ion-chromatographic analysis is its ability to analyze all cationic and anionic species in only two separate runs. The concentrations of ionic species were determined by comparing peak areas of test solutions with those of standard solutions for each species, then determining the concentrations corresponding to the area of the unknown ionic species. This analytical method has the additional advantage of identifying ionic species from the retention times of various peaks observed in the chromatograms. The cations analyzed included $Na^+$, $Ca^{2+}$, and $TBP^+$ (tetrabutyl phosphonium) and $TEP^+$ (tetraethyl phosphonium); the anions studied were $Cl^-$, $Br^-$, $NO_2^-$, $MoO_4^{2-}$), and $SO_4^{2-}$.

## Analysis of Disk Samples for Presence of Ionic Species Following Electromigration

During electromigration, cationic inhibitors move toward the cathode (negative) compartment and anionic inhibitors move toward the anode (positive) compartment. Some of the inhibitor species remain in the concrete disk. To determine the inhibitor ion content in the disk, we crushed and ground a core sample of the disk. A 5-g sample of the ground disk was heated for 1 hour in 100 mL of water at 80°-90°C. During this period, soluble cationic and anionic species were leached into the solution. The resulting water extract of the core sample was analyzed for cationic and anionic species to determine the inhibitor ion concentration. From this concentration, we can determine the total inhibitor content present in the entire disk, assuming its uniform distribution within the disk.

# 4

# Inhibitor Injection Studies

All experiments were performed with concrete columns or blocks. Columns were 2 in. in diameter and 8 in. tall, and blocks measured 18 x 3 x 2 in. Rebars were placed lengthwise in the blocks 2 in. below the top surface. Some rebar samples with a cross-sectional area of 1.33 $cm^2$ were also placed in these blocks for small-scale studies when necessary. For the inhibitor injection studies, glass cylinders 2 in. in diameter were placed on the top surface of the concrete blocks to allow inhibitor injection.

To determine the effectiveness of $TEPNO_2$ as a corrosion inhibitor for rebar steel embedded in concrete, we prepared three concrete columns containing 15 $lb/yd^3$ of $Cl^-$ with steel samples embedded in them. One column had no inhibitor, the second column had an equivalent of 50 mM $TEPNO_2$ added to the water used for making concrete, and the third column had a patented inhibitor formulation added to the water. The latter formulation was composed of 7.25 mM $NaNO_2$ (500 ppm), 0.53 mM sodium glycinate (50 ppm), and 1.93 mM hydrazine hydrate (100 ppm). The corrosion potentials and the corrosion rates exhibited by the embedded steel rebar samples in the three concrete columns were compared to determine the relative effectiveness of $TEPNO_2$ and the patented inhibitor formulation.

In another set of experiments, the $TEPNO_2$ inhibitor was injected by applying an electrical field across the top and bottom of concrete columns. The electrodes used were DSA materials supplied by ELTECH Research Corporation. In all cases, the columns were placed in a solution of saturated $Ca(OH)_2$ and the solution on the top of the column was saturated $Ca(OH)_2$ containing 100 mM of tetraethylphosphonium nitrite $TEPNO_2$.

When the electrical field is applied, the inhibitor cations ($TEP^+$) are expected to move toward the interior of the columns. Once a sufficient amount of the inhibitor cations reaches the rebar steel surface, inhibition of steel corrosion occurs and can be detected by either a lowered corrosion rate or a shift of the corrosion potential in the positive direction. Thus, as the inhibitor injection time is increased, the corrosion potential should move in the positive direction until maximum achievable steel corrosion inhibition occurs.

AC impedance spectroscopy was used to determine the in situ corrosion rates of rebar samples embedded in concrete columns containing 15 lb/yd$^3$ of $Cl^-$ ions. This technique has the advantage of allowing measurement of the corrosion rate of the rebar steel while the inhibitor is being injected. The corrosion potential of the steel specimens was also monitored while the inhibitor was being injected.

When the inhibitor was injected into concrete blocks (18 x 3 x 2 in.), it was first applied on the top surface of each block; a sponge saturated with calcium hydroxide was then placed to cover the entire top surface. A DSA™ was laid on the upper surface of the sponge, and the electrical field was applied across this anode and the rebar cathode. The sponge had to be kept moist for optimal inhibitor injection (see Figure 4-1).

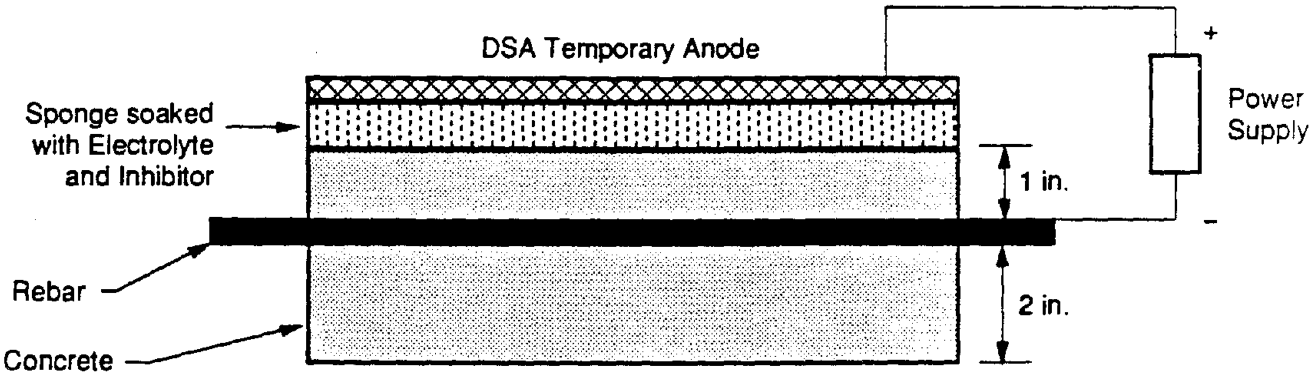

Figure 4-1. Experimental Arrangement used for Corrosion Inhibitor Injection into Concrete Blocks.
(Block dimensions: 18 in. x 3 in. x 2 in.)
(1 in. = 2.54 cm)

# 5

# Results and Discussion

## Quaternary Ammonium Inhibitors

The quaternary ammonium compounds investigated included tetramethyl and tetrabutyl quaternary ammonium salts with the counteranions $NO_2^-$, and $MoO_4^{2-}$. With the smaller tetramethyl cation, the nitrite analog showed better inhibition than the molybdate analog, whereas with the larger tetrabutyl cation, the situation was reversed.

The corrosion inhibition data obtained with quaternary ammonium inhibitors are summarized in Table 5-1.

## Quaternary Phosphonium Inhibitors

Because quaternary ammonium inhibitors did not seem very effective as corrosion inhibitors for steel in 5% NaCl (pH = 10.5), we decided to synthesize quaternary inhibitors based on the phosphonium cations. The results were encouraging: the phosphonium compounds (Table 5-2) in general, outperformed the corresponding ammonium compounds.

Figure 5-1 shows a comparison of the Nyquist plots of the steel/solution interfacial impedance in 5% NaCl (pH = 10.5) in the presence of the inhibitors tetrabutylammonium molybdate and tetrabutylphosphonium molybdate. Clearly, phosphonium molybdates provide superior corrosion inhibition than the ammonium molybdates. Thus, we concluded that in alkaline environments

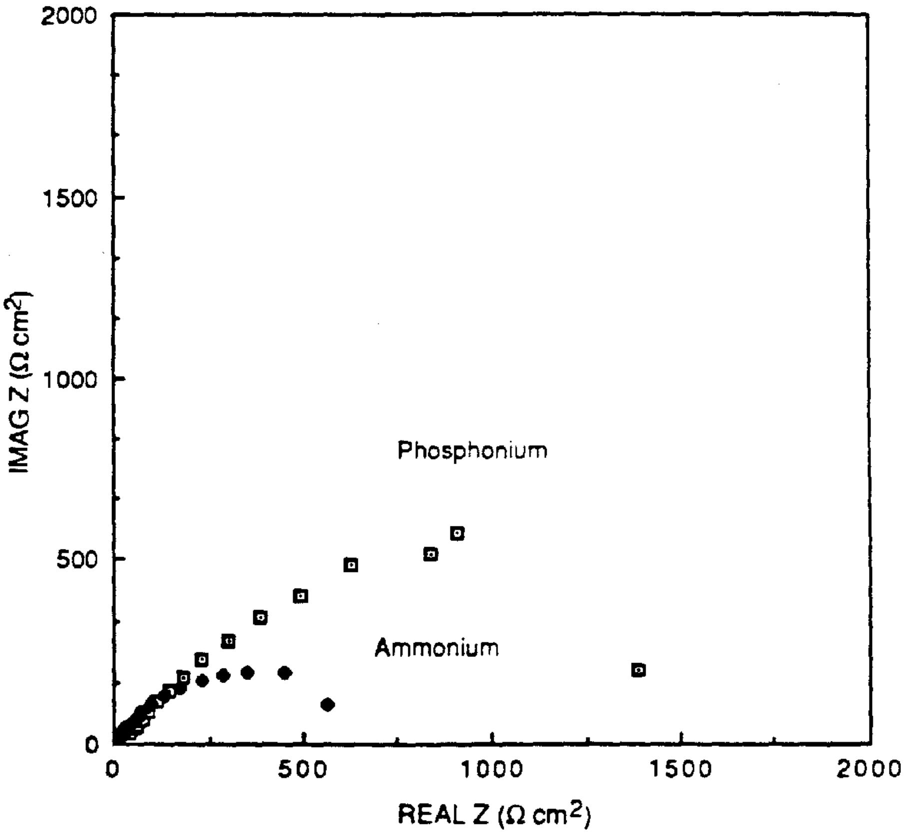

Figure 5-1. Nyquist plots of the steel/solution interface in 5% NaCl (pH = 10.5) demonstrating the influence of the type of cation on $R_p$ values.

◆ Tetrabutylammonium molybdate (10 mM)
◘ Tetrabutylphosphonium molybdate (10 mM)
T = 298 K, ω = 500 rpm

Table 5-1. Summary of corrosion inhibition data for rebar steel in the presence of quaternary ammonium inhibitors

| System | $E_{corr}$ (V) SCE | $R_p$ ($\Omega$ cm$^2$) | Efficiency (%) |
|---|---|---|---|
| S: 5% NaCl (pH = 10.5) | -0.540 | 228 | – |
| S + 10 mM Tetramethyl-ammonium nitrite | -0.466 | 717 | 68 |
| S + 10 mM Tetramethyl-ammonium molybdate | -0.469 | 493 | 54 |
| S + 10 mM Tetrabutyl-ammonium nitrite | -0.478 | 392 | 42 |
| S + 10 mM Tetrabutyl-ammonium molybdate | -0.457 | 663 | 66 |

corrosion inhibitors based on quaternary phosphonium salts are better than those based on the corresponding ammonium salts in alkaline environments.

Experiments were performed with tetrabutylphosphonium cations having the supporting anions bromide (smallest), nitrite (intermediate), and molybdate (largest). Molybdate provides better inhibition than nitrite, and nitrite provides better inhibition than bromide. Thus, the corrosion inhibition efficiency is related to anion size: the larger the anion, the higher the corrosion inhibition efficiency with a given cation. Accordingly, the $R_p$ varies in the following manner.

$$R_p\,(MoO_4^{2-}) > R_p\,(NO_2^-) > R_p\,(Br^-) \qquad (5.1)$$

We believe this trend is due to the higher polarizability of the larger anions, which adsorb strongly onto metal surfaces and promote the subsequent adsorption of quaternary inhibitor cations, thus resulting in higher inhibition efficiencies.

A complete summary of the $R_p$ and corrosion inhibitor efficiency data of compounds evaluated during this study appears in Table 5-2. Clearly, a number of candidate materials among the quaternary compounds proved extremely promising. They are tetramethylphosphonium molybdate, tetraethylphosphonium molybdate, tetrabutylphosphonium molybdate, and tetraphenylphosphonium nitrite, with efficiencies in the range of 85% to 92%. Because of our considerable success with the synthesis of new phosphonium-based quaternary inhibitors that perform well in alkaline chloride environments, we believe that we have discovered a unique group of corrosion inhibitors that can be injected into concrete to prevent steel rebar corrosion.

Table 5-2. Summary of corrosion inhibition data for rebar steel in the presence of inhibitors studied

| System | $E_{corr}$ (V) SCE | $R_p$ ($\Omega$ cm$^2$) | Inhibitor Efficiency (%) |
|---|---|---|---|
| S: 5% NaCl (pH = 10.5) | - 0.540 | 228 | – |
| S + 10 mM Tetramethyl-ammonium nitrite | - 0.466 | 717 | 68 |
| S + 10 mM Tetramethyl-ammonium molybdate | 0.469 | 493 | 54 |
| S + 10 mM Tetrabutyl-ammonium nitrite | - 0.478 | 392 | 42 |
| S + 10 mM Tetrabutyl-ammonium molybdate | - 0.457 | 663 | 66 |
| S + 10 mM Tetramethyl-phosphonium nitrite | - 0.468 | 610 | 63 |
| S + 10 mM Tetramethyl-phosphonium molybdate | - 0.464 | 1559 | 85 |
| S + 10 mM Tetraethyl-phosphonium nitrite | - 0.467 | 1022 | 78 |
| S + 10 mM Tetraethyl-phosphonium molybdate | - 0.436 | 2809 | 92 |
| S + 10 mM Tetrabutyl-phosphonium nitrite | - 0.465 | 859 | 73 |
| S + 10 mM Tetrabutyl-phosphonium molybdate | - 0.443 | 1755 | 87 |
| S + 10 mM Tetraphenyl-phosphonium nitrite | - 0.453 | 1499 | 85 |
| S + 10 mM Tetraphenyl-phosphonium molybdate | - 0.482 | 275 | 17 |

## Optimization of Inhibitor Cation Injection

One of the important objectives of this research was to optimize the electrical conditions required for inhibitor injection before actual testing was performed with concrete blocks. To achieve this objective, we chose to use cured mortar disks. The degree of optimization was decided on the basis of the transport number and the electromigrated amount of inhibitor cations under a given set of experimental conditions. Thus, both the transport number and the electromigrated inhibitor content were determined as a function of the applied field, current, and the duration of electromigration tests. In principle, the transport number is not expected to vary over time, unless the interaction between the mortar matrix and the inhibitor cation changes, because of such effects as surface etching, pore blocking, or pore widening. However, the electromigrated inhibitor content increases with time and reaches a limiting value because of the gradual decrease in concentration on the side initially containing the inhibitor. Thus, a study of the inhibitor injection rate as a function of applied field and current density provides valuable information on the optimized conditions of the latter parameters for efficient inhibitor injection.

Tables 5-3 through 5-5 summarize the transport numbers of tetrabutylphosphonium cations at different experimental times and average currents at applied electrical fields of 5, 10, and 20 V/cm. Transport numbers of the electromigrating phosphonium cations ($t_{p+}$) were determined using the following expression.

$$t_{p+} = \frac{Q_{p+}}{Q_{Total}}$$

where $Q_{p+}$ is the charge carried by phosphonium cations and $Q_{Total}$ is the total charge passed over a given period of time. $Q_{p+}$ is evaluated by determining the concentration buildup of phosphonium cations in the inhibitor-free side and converting this concentration to the equivalent number of coulombs by using Faraday's law.

## Transport Numbers of TBP$^+$ Cation

Table 5-3 shows that, when the electrical field is 5 V/cm, the transport number of TBP$^+$ ions varies in the range 0.0057 to 0.0065 up to 120 hours, whereas during the period from 120 to 195 hours, the transport number drops from 0.0061 to 0.0038 a 38% reduction. However, the decrease in average current during this period is only 6%. Thus, the large reduction in the transport number is attributed to the decreased concentration of TBP$^+$ cations on the anode side and the greater interaction of these cations with the cement matrix at longer times. Thus, Table 5-3 that the optimum transport number for TBP$^+$ ions is achieved in 120 hours and continued electromigration beyond that time without cation replenishment on the anode side results in a considerable reduction in their transport number.

Table 5-3. Summary of Transport Number Data for $TBP^+$ ions at 5 V (DC)

| Time (hr) | Average Current Density ($mA/cm^2$) | Transport Number for $TBP^{\pm}$ |
|---|---|---|
| 0 | 1.10 | - |
| 24 | 1.03 | - |
| 49 | 0.92 | 0.0058 |
| 74 | 0.84 | 0.0057 |
| 100 | 0.79 | 0.0065 |
| 120 | 0.76 | 0.0061 |
| 195 | 0.71 | 0.0038 |

Electrolyte: Saturated $Ca(OH)_2$.
Inhibitor: 100 mM $TBPNO_2$.
1 $mA/cm^2$ = 0.9 A/sq. ft.

Table 5-4 shows a summary of the transport number data for $TBP^+$ cations through the cement matrix at an applied field of 10 V/cm. The transport number in this case is approximately twice as high because of the increased field. Table 5-5 illustrates that the transport number of $TBP^+$ cation can be increased by another 30-40% by increasing the field from 10 to 20 V/cm. This field-dependent transport number for cations may be associated with the cationic binding sites in the matrix.

Table 5-4. Summary of Transport Number Data For $TBP^+$ ions at 10 V (DC)

| Time (hr) | Average Current Density ($mA/cm^2$) | Transport Number for $TBP^+$ |
|---|---|---|
| 0 | 1.39 | - |
| 24 | 1.31 | - |
| 48 | 1.26 | 0.013 |
| 72 | 1.19 | 0.010 |
| 96 | 1.13 | 0.008 |
| 120 | 1.08 | 0.007 |

Electrolyte: Saturated $Ca(OH)_2$.
Inhibitor: 100 mM $TBPNO_2$.
1 $mA/cm^2$ = 0.9 A/sq. ft.

Table 5-5. Summary of Transport Number Data for $TBP^+$ 20 V (DC)

| Time (hr) | Average Current Density ($mA/cm^2$) | Transport Number for $TBP^+$ |
|---|---|---|
| 0 | 2.74 | – |
| 24 | 2.82 | 0.018 |
| 48 | 2.53 | 0.013 |
| 72 | 2.34 | 0.012 |
| 96 | 2.19 | 0.008 |
| 120 | 2.06 | 0.006 |

Electrolyte: Saturated $Ca(OH)_2$.
Inhibitor: 100 mM $TBPNO_2$.
1 $mA/cm^2$ = 0.9 A/sq. ft.

Comparison of the transport numbers beyond 96 hours at fields of 5, 10, and 20 V/cm indicates that they reach a field-independent value at and beyond 10 V/cm. However, at the lower field of 5 V/cm, the transport number for $TBP^+$ ions remains steady in the range 0.0057 to 0.0065 for 120 hours. The field independence is presumably due to the rapid transport of $TBP^+$ ions at higher fields at shorter times, followed by its slower transport at longer times as a result of side reactions, such as oxygen evolution at the anode, that override the transport of inhibitor cations. Oxygen evolution results in a reduction in pH on the anode side at high fields, which must be buffered by the periodic addition of $Ca(OH)_2$ to this side to maintain the pH around 11. This side reaction can be minimized in several ways, including reducing the applied field, using an anode material with a higher oxygen overvoltage, or periodically replenishing the $TBP^+$ concentration on the anode side to prevent or minimize concentration polarization effects.

From these results it appears that effective transport of $TBP^+$ through cement mortar matrices can be achieved at an applied electrical field of 5 V/cm. Furthermore, the lower current densities, reduced gas evolution, and minimum pH changes observed indicate that the conditions for transport of $TBP^+$ ions are optimized at an applied field of 5 V/cm despite the lower transport numbers observed for $TBP^+$ ion migration.

## Transport Numbers of $TEP^+$ Cation

Tables 5-6 through 5-8 summarize the transport number data for $TEP^+$ cations at applied electrical fields of 5, 10, and 20 V/cm.

Table 5-6. Summary of Transport Number data for $TEP^+$ ions at 5 V (DC)

| Time (hr) | Average Current Density ($mA/cm^2$) | Transport Number for $TEP^+$ |
|---|---|---|
| 0 | 0.76 | - |
| 24 | 0.69 | 0.053 |
| 49 | 0.63 | 0.046 |
| 74 | 0.58 | 0.042 |
| 100 | 0.53 | 0.035 |
| 120 | 0.50 | 0.033 |
| 195 | 0.45 | 0.020 |

Electrolyte: Saturated $Ca(OH)_2$.
Inhibitor: 100 mM $TEPNO_2$.
1 $mA/cm^2$ = 0.9 A/sq. ft.

Table 5-7. Summary of Transport Number Data for $TEP^+$ ions at 10 V (DC)

| Time (hr) | Average Current Density ($mA/cm^2$) | Transport Number for $TEP^+$ |
|---|---|---|
| 0 | 1.77 | - |
| 20 | 1.77 | 0.058 |
| 44 | 1.65 | 0.047 |
| 100 | 1.50 | 0.025 |
| 120 | 1.39 | 0.021 |

Electrolyte: Saturated $Ca(OH)_2$.
Inhibitor: 100 mM $TEPNO_2$.
1 $mA/cm^2$ = 0.9 A/sq. ft.

Table 5-8. Summary of Transport Number Data for $TEP^+$ ions at 20 V (DC)

| Time (hr) | Average Current Density ($mA/cm^2$) | Transport Number for $TEP^+$ |
|---|---|---|
| 0 | 2.90 | – |
| 20 | 3.23 | 0.040 |
| 44 | 2.85 | 0.034 |
| 100 | 2.55 | 0.016 |
| 120 | 2.31 | 0.016 |

Electrolyte: Saturated $Ca(OH)_2$.
Inhibitor: 100 mM $TEPNO_2$.
1 $mA/cm^2$ = 0.9 A/sq. ft.

Transport numbers for $TEP^+$ cations are approximately an order of magnitude higher than the corresponding numbers for $TBP^+$ cations at 5 V/cm. At higher electrical fields (10 and 20 V/cm), $t_{TEP+}$ is approximately 3-4 times higher than $t_{TBP}{}^+$. The variation of $t_{TBP}{}^+$ over time at 5, 10, and 20 V/cm is similar to the corresponding variation observed for $t_{TEP}{}^+$. An interesting feature observed with $TEP^+$ is that the applied electrical field has very little influence on $t_{TEP}{}^+$. No increase in transport number was observed with increases in applied voltage. Even with $TEP^+$, the most desirable electrical condition for inhibitor cation injection appears to be a field of 5 V/cm. The low applied electrical field has the advantage of maintaining a constant pH and minimizing side reactions that lead to gas evolution.

A blank experiment was conducted with the two-compartment cell separated by a 1-cm-thick cement disk. One compartment contained a saturated solution of $Ca(OH)_2$, and the other contained 100 mM of $TEPNO_2$ dissolved in a saturated solution of $Ca(OH)_2$. The cell was allowed to stand without the application of an electrical field to determine the transport properties of $TEP^+$ cation in the absence of an electrical field. Analysis of the initially inhibitor-free side of the cell showed the absence of $TEP^+$ ionic species even after 19 days of simple diffusion. This result proves that the inhibitor ion transport we observed is entirely electrical field-assisted.

## Electrical Injection of $TBP^+$ and $TEP^+$ Cations (as 100 mM Solution)

We have shown the possibility of electrically injecting $TBP^+$ cations through a mortar matrix. In this study, we performed experiments to determine the contents of electrically transported inhibitor cations at applied fields of 5, 10, and 20 V/cm. The mortar samples were each 4 cm in diameter and 1 cm thick. The results are shown in Figure 5-2. Clearly, the injected $TBP^+$ concentration increases with time in all cases and reaches a limiting value after approximately 96 hours, the plateau concentrations being higher with higher applied electrical fields.

Figure 5-3 shows the results of an identical study performed with the smaller inhibitor cation $TEP^+$. Clearly, cation injection is faster with $TEP^+$ than with $TBP^+$. Plateau concentrations of

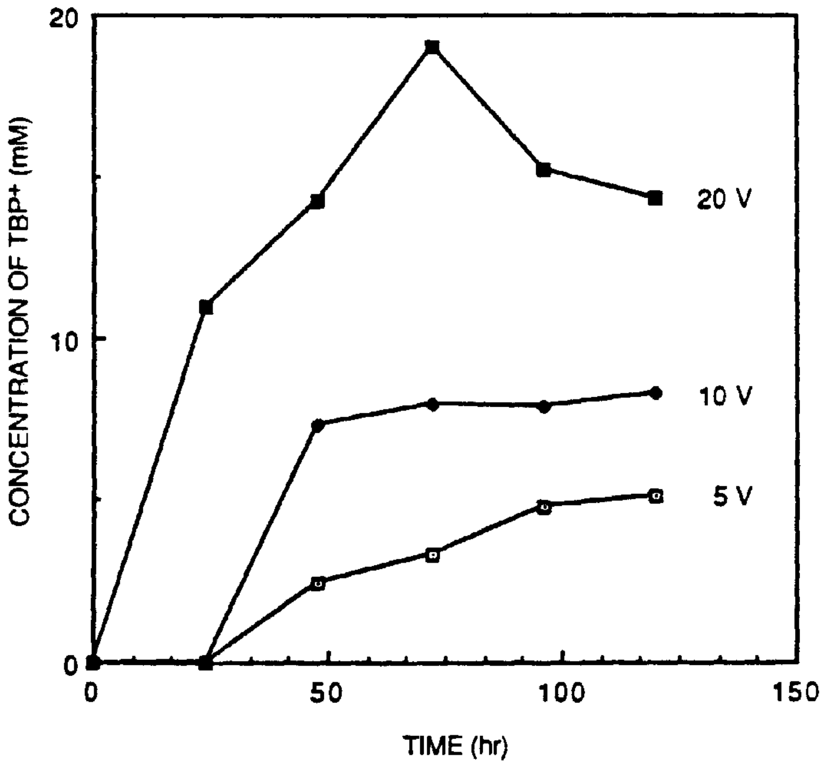

Figure 5-2. Variation of the concentration of electrically injected $TBP^+$ cation as a function of time at different applied voltages.

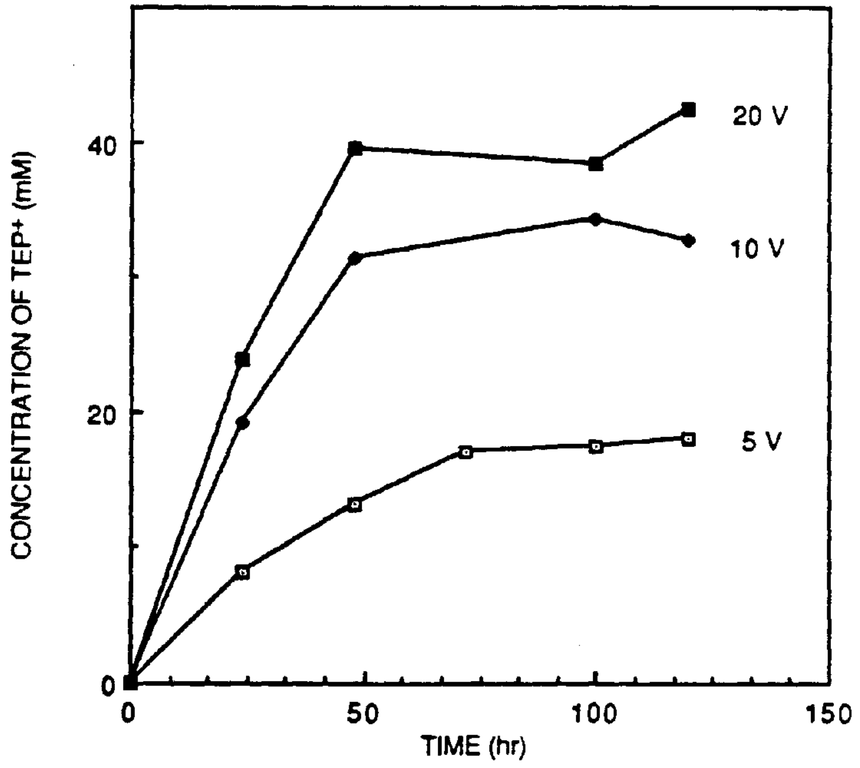

Figure 5-3. Variation of the concentration of electrically injected $TEP^+$ cation as a function of time at different applied voltages.

$TEP^+$ at 120 hours are at least 3-4 times higher than the corresponding applied concentrations of $TBP^+$ at selected fields. Thus, with the same field over the same period of time, it is possible to inject 4 times more $TEP^+$ than $TBP^+$. Higher concentrations are achievable with $TEP^+$ because its transport number is higher than that of $TBP^+$. Thus, electrical injection of $TEP^+$ appears to be more efficient than that of $TBP^+$.

To determine whether anionic movement occurs with the injection of $TBP^+$ and $TEP^+$ cations, we analyzed the disk samples at the end of the experiments. The samples were crushed, extracted with 100 mL of water at 90°C, and analyzed for the presence of $NO_2^-$ and $NO_3^-$ ions. With both inhibitors, anionic movement into the mortar disks had taken place. The $NO_2^-$ anion had undergone oxidation to $NO_3^-$, and its content in the disk varied from 0.0077 mol to 0.0217 mol over the test period. This result proves that along with the cationic inhibitor injection, some anionic movement also occurs, presumably because of the electrophoretic effect. Thus, we may be able to use a stable anionic species other than $NO_2^-$ (which would also have a corrosion inhibiting effect) as the counteranion.

When molybdate anion was used with the inhibitor cation in inhibitor injection studies, it appeared to undergo an oxidative reaction at the anode, causing precipitation of the quaternary salt. Thus, the preferred anion in all inhibitor injection studies was the nitrite ion.

## Inhibitor Injection into Mortar Matrices

Experiments were performed with 2-cm-thick mortar disks to determine the rate of injection of $TEP^+$ ions into mortar matrices. The disks had been cured for 28 days. The results of the electrical injection of $TEP^+$ inhibitor cations through mortar disks at applied fields of 5, 10, and 20 V/cm are shown in Figure 5-4. Clearly, the transport of $TEP^+$ ions through mortar is faster at higher applied fields. However, higher applied fields (e.g., 20 V/cm) also increase the acidity on the anode side, which must be neutralized periodically by adding $Ca(OH)_2$ to maintain the pH at a constant value. Hence, pH changes in the anode side at lower applied fields (e.g., 5 V/cm) are smaller and beneficial in preventing surface etching of the mortar disk. It appears likely that a field of 5 V/cm would be adequate for injection of $TEP^+$ cations into mortar matrices if injection time is not a major constraint. If short-time inhibitor injections are required, a good compromise would be a field of 10 V/cm with adequate neutralization of acidity on the anode side with the addition of $Ca(OH)_2$.

## Inhibitor Injection into Concrete Matrices

Figure 5-5 shows the rate of injection of $TEP^+$ cations into concrete matrices at applied fields of 5, 10, and 20 V/cm. The concrete disks were 2 cm thick and had been cured over a 28-day period. Once again it is clear that $TEP^+$ inhibitor cations move faster at higher applied fields. Comparing Figures 5-4 and 5-5 shows that transport of inhibitor cations occurs more slowly through concrete than through cement, except when the applied field is 5 V/cm. We cannot explain this apparent inversion at this time. However, the slower transport of inhibitor cations through the concrete

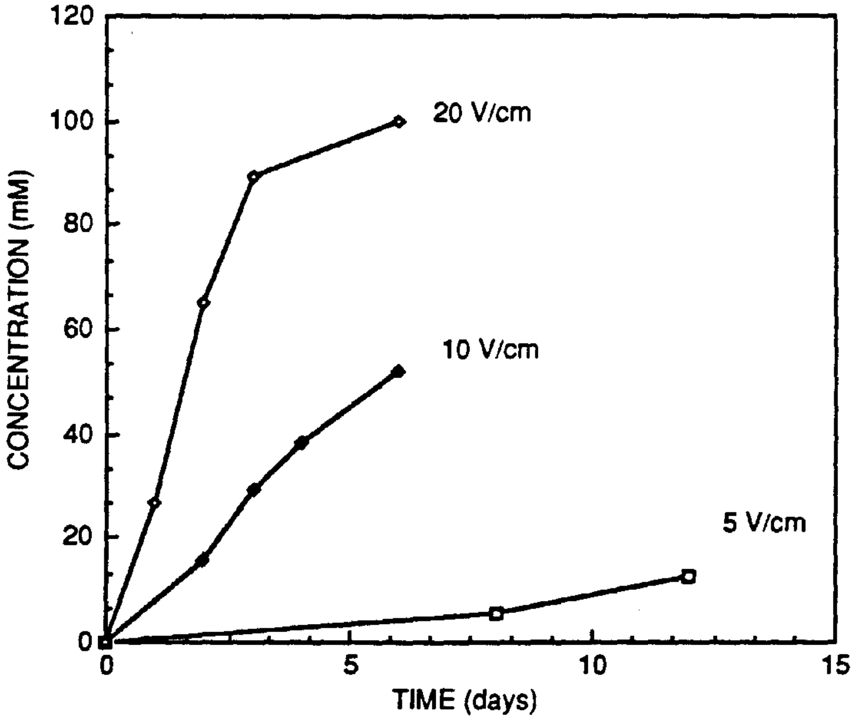

Figure 5-4. Variation of the concentration of electrically injected $TEP^+$ cations through mortar as a function of time at different applied fields.

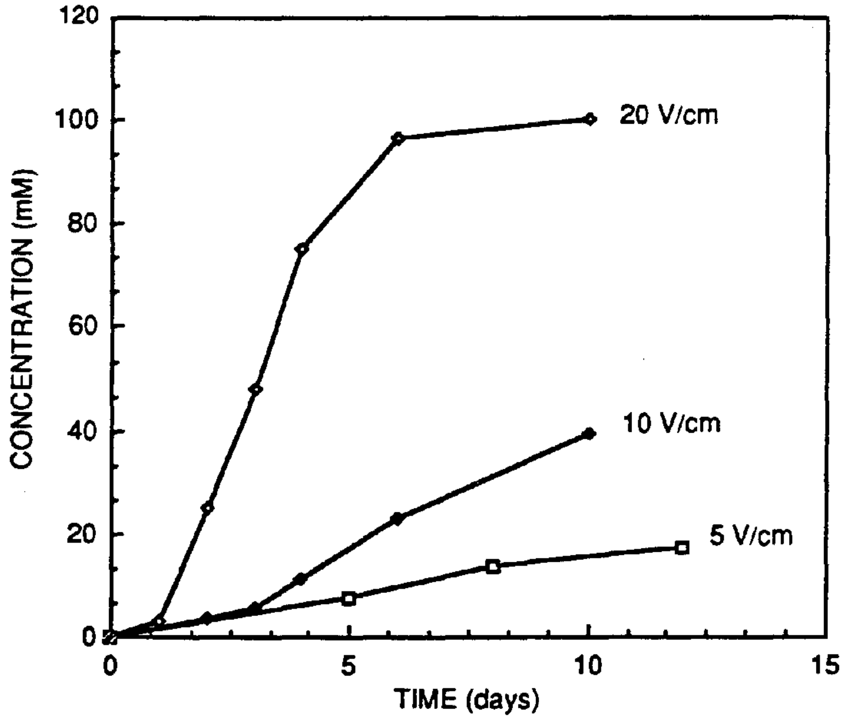

Figure 5-5. Variation of the concentration of electrically injected $TEP^+$ cations through concrete as a function of time at different applied fields.

matrix is expected because of the aggregate in the matrix, which considerably reduces the area available for ionic transport. Despite this obstacle, considerable inhibitor injection occurs through the concrete matrix at 10 and 20 V/cm over a 6-day injection period. For example, in 6 days the inhibitor ionic transport to the cathode side is 23% with a field of 10 V/cm, but 96% with a field of 20 V/cm. Thus, although somewhat slower, inhibitor ionic transport through concrete matrices by an electrical field-assisted approach is completely feasible within a realistic time frame.

### Transport Numbers of $TEP^+$ Cation Through Concrete Matrices

Table 5-9 shows the transport number data for $TEP^+$ cations through concrete at applied electrical fields of 5, 10, and 20 V/cm, using 2-cm-thick concrete disks cured over 28 days. Over the test period of 10-12 days, $t_{TEP^+}$ in concrete was 0.013 ± 0.001 at a field of 5 V/cm, 0.016 ± 0.003 at a field of 10 V/cm, and 0.029 ± 0.003 at a field of 20 V/cm. Thus, the transport number increased by 23% when the field was increased from 5 to 10 V/cm and by 81% when the field was increased from 10 to 20 V/cm. We attribute this field-dependent transport number to cationic binding sites in the concrete.

A comparison of the transport number data for mortar (Tables 5-6 through 5-8) and concrete (Table 5-9) indicates that the transport number remains approximately the same at long times for both matrices at 10 V/cm, whereas at 20 V/cm the transport numbers for $TEP^+$ in concrete are marginally higher. At a given applied field, the current density observed with mortar is approximately the same as that observed with concrete. This observation, when considered along with the somewhat similar transport numbers observed with both mortar and concrete matrices, indicates that the transport number is not strongly affected by the nature of the matrix (i.e., mortar or concrete).

The inhibitor injection rate ($Q^+$ vs. time) determined from Table 5-9 indicates that the rate in general increases linearly as the current densities increases. The results further indicate that the inhibitor injection rate increases in the order 35, 95 and 420 $\mu g/cm^2/hr$ at current densities of 0.5-0.65, 0.9-1.04 and 2.1-2.9 $mA/cm^2$. Thus, doubling the current density increases the inhibitor injection rate by approximately 3 to 4 times. A current density of 1 to 2 $mA/cm^2$ appears to be the best under the conditions studied, however, to avoid damage to concrete a current density of < 1 $mA/cm^2$ would be more appropriate.

Table 5-9. Summary of Transport Number Data for $TEP^+$ ions through Concrete

| Time (hr) | Average Current Density ($mA/cm^2$) | Charge Carried by $TEP^+$ Ions ($Q^+$) $C/cm^2$ | Transport Number for $TEP^+$ |
|---|---|---|---|
| Field of 5 V/cm | | | |
| 0 | 0.72 | | – |
| 25 | 0.70 | | – |
| 118.5 | 0.63 | 2.956 | 0.011 |
| 192.5 | 0.57 | 5.135 | 0.013 |
| 286.5 | 0.46 | 6.64 | 0.014 |
| Field of 10 V/cm | | | |
| 0 | 1.24 | | – |
| 19.5 | 1.16 | | – |
| 49.5 | 1.09 | 1.40 | 0.0072 |
| 69 | 1.04 | 2.22 | 0.0086 |
| 93.5 | 1.00 | 4.37 | 0.013 |
| 144 | 0.98 | 9.14 | 0.018 |
| 240.5 | 0.90 | 14.80 | 0.019 |
| Field of 20 V/cm | | | |
| 0 | 3.24 | | – |
| 19.5 | 2.88 | 1.11 | 0.0055 |
| 49.5 | 3.00 | 9.62 | 0.018 |
| 69 | 2.91 | 18.80 | 0.026 |
| 93.5 | 2.69 | 28.97 | 0.032 |
| 144 | 2.42 | 37.64 | 0.030 |
| 240.5 | 2.11 | 47.50 | 0.026 |

Disk: Concrete (2 cm thick.)
Electrolyte: Saturated $Ca(OH)_2$.
Inhibitor: 100 mM $TEPNO_2$.
1 $mA/cm^2$ = 0.9 A/sq. ft.

## Effectiveness of $TEPNO_2$ as a Corrosion Inhibitor for Rebar Steel Embedded in Concrete

Corrosion rates and corrosion potentials of rebar steel embedded in chloride-containing (15 $lb/yd^3$) concrete columns with and without inhibitors were monitored over two months to determine the effectiveness of $TEPNO_2$ as a corrosion inhibitor for rebar steel. Two inhibitors were compared: (1) 50 mM $TEPNO_2$ and (2) a mixture of 7.25 mM $NaNO_2$ (500 ppm), 0.53 mM sodium glycinate (50 ppm), and 1.93 mM hydrazine hydrate (100 ppm). Each inhibitor was applied by adding it to the water used for mixing concrete.

The potentials were measured after the concrete columns were allowed to cure for five weeks. After that time, the steel in the concrete without the inhibitor showed a potential of -0.457 V with respect to an Ag/AgCl, 0.1 M KCl reference electrode. Steel embedded in columns containing TEPNO$_2$ and the NO$_2^-$/glycinate/hydrazine hydrate mixture showed potentials of -0.001 and 0.000 V, respectively. Both inhibitors increased the potential of the steel sample to almost the same value, which indicates that TEPNO$_2$ is as effective as the complex inhibitor formulation consisting of NO$_2^-$, glycinate, and hydrazine hydrate. Table 5-10 shows the variation in corrosion potential ($E_{corr}$) over time for the steel samples embedded in concrete with and without the inhibitors, TEPNO$_2$ and the NO$_2^-$/glycinate/hydrazine hydrate mixture (M). Clearly, in all cases the potential becomes more negative over time up to a point, then tends to increase slightly. Further potential measurements are needed before it is possible to conclude whether this slight increase is valid. Nevertheless, Table 5-10 clearly shows that the potential of the steel is more positive by 0.150-0.200 V with the inhibitors. This finding indicates that these inhibitors provide almost the same extent of protection to the steel.

Table 5-10. Influence of TEPNO$_2$ and the Inhibitor Mixture M* on the corrosion potential of steel embedded in concrete containing 15 lb/yd$^3$ of Cl$^-$ ions

| Time | | | $E_{corr}$ (V) |
|---|---|---|---|
| (weeks) | Blank | TEPNO$_2$ | M |
| 5 | - 0.457 | - 0.001 | 0.000 |
| 6.5 | - 0.595 | - 0.231 | - 0.491 |
| 8.5 | - 0.584 | - 0.369 | - 0.440 |
| 10 | - 0.552 | - 0.331 | - 0.399 |

*M: NO$_2^-$/glycinate/hydrazine hydrate mixture (a patented inhibitor formulation)
Disk: Mortar (2 cm)
Electrolyte: Saturated Ca(OH)$_2$
Inhibitor: 100 mM TEPNO$_2$

An AC impedance study made on the steel samples showed an $R_p$ value of 865 Ω cm$^2$ for the inhibitor-free samples, followed by a Warburg impedance characteristic of oxygen diffusion into the concrete matrix. With the two inhibitor formulations, TEPNO$_2$ and M, the impedance spectra showed two successive relaxations in both cases. These relaxations correspond to resistive impedances of 3800, 3200 Ω cm$^2$ and 2400, 4375 Ω cm$^2$, respectively. With the limited time available, it was not possible to undertake a complete mechanistic diagnosis of these relaxations. However, we believe the first relaxation is due to a film on the surface of the metal and the second, at lower frequencies, corresponds to the $R_p$. Thus, we must compare the $R_p$ value of 865 Ω cm$^2$ for the inhibitor-free case with the values of 3200 Ω cm$^2$ observed with TEPNO$_2$ and 4375 Ω cm$^2$ observed with M. This result means that the corrosion rate with the inhibitors TEPNO$_2$ and M has been reduced by approximately 73-80%.

Previously we showed that steel embedded in mortar had an $R_p$ value of 3525 $\Omega$ $cm^2$ in the presence of 15 $lb/yd^3$ of $Cl^-$ ions. In the present case, steel embedded in concrete had an $R_p$ value of 865 $\Omega$ $cm^2$ in the presence of the same $Cl^-$ ion content. These two results indicate that corrosion rate of steel embedded in concrete is approximately 4 times higher than that of steel embedded in mortar. The difference may be related to oxygen diffusing through concrete faster than through mortar.

## Inhibitor Injection into Mortar and Concrete Columns

We performed preliminary studies on corrosion inhibitor injection into mortar as well as into concrete columns by an electrical field assisted approach. The mortar had a cement:sand:water composition of 1:3:0.5, whereas the concrete had a cement:sand:aggregate:water composition of 1:2.2:2.75:0.5. Size 4 aggregates were used in making concrete disks and columns. Both types of columns had 15 $lb/yd^3$ of $Cl^-$ ions and had been cured over 28 days. For comparison, we also made a mortar column 8 in. high with no added $Cl^-$ All columns had rebar steel samples embedded 2 in. from the top, and some had a second rebar steel sample 7 in. from the top. The area of the steel samples was 1.33 $cm^2$.

We measured the $E_{corr}$ of steel rebar samples and estimated their corrosion rates using AC impedance spectroscopy as a function of inhibitor injection time. The inhibitor was injected by applying an electrical field across the top and bottom of the mortar or concrete columns. The electrodes were DSA™ materials supplied by ELTECH Research Corporation. The columns were placed in a solution of saturated $Ca(OH)_2$ in all cases, and the solution on the top of each column was 5% NaCl (pH 10), saturated $Ca(OH)_2$, or saturated $Ca(OH)_2$ containing 100 mM solution of $TEPNO_2$.

When the electrical field is applied, the inhibitor cations ($TEP^+$) are expected to move toward the interior of the columns. Once a sufficient amount of the inhibitor cations reaches the rebar steel surface, inhibition of steel corrosion occurs and can be detected by either a lowered corrosion rate or a shift of the $E_{corr}$ in the positive direction. Thus, as the inhibitor injection time is increased, the $E_{corr}$ should move in the positive direction until maximum achievable steel corrosion inhibition occurs.

The preliminary results performed with a mortar column without $Cl^-$ ions showed an $R_p$ value of 66,500 $\Omega$ $cm^2$, whereas in the presence of $Cl^-$, the $R_p$ value dropped to 3525 $\Omega$ $cm^2$. Because $R_p$ is inversely related to the corrosion rate, the reduced $R_p$ indicates an approximately 20-fold increase in the corrosion rate of the rebar steel in mortar containing 15 $lb/yd^3$ of $Cl^-$ ions. The inhibitor injection study was performed with a mortar column containing $Cl^-$ ions. The inhibitor used was 100 mM $TEPNO_2$, and the field applied was 5 V/cm. After 138 hours (almost 6 days) of inhibitor injection, the $R_p$ value increased from 3525 $\Omega$ $cm^2$ to 18,000 $\Omega$ $cm^2$, which is an approximately 5-fold increase in $R_p$. Furthermore, the $E_{corr}$ of the rebar steel measured against a Ag/AgCl, 0.1 N KCl reference electrode increased from -0.465 V to -0.227 V. Thus, the system showed a lower corrosion rate and a 0.238 V shift of the $E_{corr}$ in the positive direction. Both these factors indicate the inhibition of rebar steel corrosion. In fact, after 11-1/2 days of inhibitor injection, the $E_{corr}$

shifted to an even more positive value, -0.192 V. This value must be compared with the $E_{corr}$ value of -0.104 observed for the rebar steel surface embedded in the mortar column without $Cl^-$ ions. The shift of $E_{corr}$ in the more positive direction is a clear indication of the corrosion inhibition of steel caused by the electrically injected $TEP^+$ inhibitor cation.

The next phase of study was to evaluate the efficiency of inhibitor injection into a concrete column containing 15 lb/yd$^3$ of $Cl^-$. In this study we used two concrete columns of identical chemical composition, both containing $Cl^-$ ions. Two different experiments were performed with these columns. One column had only a saturated solution of $Ca(OH)_2$, while the other had a 100-mM solution of $TEPNO_2$ in addition to $Ca(OH)_2$. When an electrical field of 5 V/cm was applied to both columns, in one case only the $Ca^{2+}$ ions could move into concrete and in the other case the inhibitor cation $TEP^+$ would move along with the $Ca^{2+}$ ions. In this way, we could determine the true influence of the inhibitor cation injection into the concrete matrix. Furthermore, this "blank" study enabled us to determine whether injection of $Ca^{2+}$ ions into concrete is beneficial for corrosion protection of steel rebars.

The results of this experiment indicate that $E_{corr}$ moves in the positive direction even with the injection of $Ca^{2+}$ ions but does not achieve a positive enough potential during the period tested. However, with the $TEP^+$ inhibitor injection, $E_{corr}$ moves to a more positive value. Thus, $E_{corr}$ without the inhibitor moved from -0.472 V (Ag/AgCl, 0.1 N KCl) to -0.314 V in 17 days of electrical field application, whereas the corresponding increase with the inhibitor was from -0.460 V to -0.196 V in 16 days. This final potential must be compared with the $E_{corr}$ of -0.104 V observed for a rebar steel in chloride-free concrete.

The fact that the $E_{corr}$ moved in the positive direction by more than 0.250 V is an extremely encouraging result, proving that the electrical inhibitor injection into concrete takes place and that the rebar steel gradually achieves a protection potential as a result. We believe it is possible to achieve an $E_{corr}$ even more positive than -0.196 V by increasing the inhibitor concentration, and increasing the applied field. Our objective is to achieve a potential as close as possible to -0.104 V, which is only 92 mV more positive than what we have achieved so far. If we can achieve an $E_{corr}$ of -0.104 V by inhibitor injection, we will have simulated a situation equivalent to a rebar steel embedded in chloride-free concrete with minimum corrosion.

We repeated this experiment to determine the degree of reproducibility of the results. The inhibitor was electrically injected into concrete columns 8 in. high. The top compartment contained 25 mL of saturated $Ca(OH)_2$ and 100 mM of $TEPNO_2$, and the bottom compartment contained only a solution of saturated $Ca(OH)_2$. The rebar steel sample was 2 in. (5 cm) below the top surface of the column. The voltage applied was 40 V, so that the applied electrical field was 5 V/cm. The $E_{corr}$ of the steel rebar sample embedded in chloride-containing concrete moved from -0.578 V to -0.168 V over 22 days of inhibitor injection. In comparison, the previously obtained result was an $E_{corr}$ variation from -0.460 V to -0.196 V in 16 days. This final potential must be compared with the $E_{corr}$ of -0.104 V observed for rebar steel in chloride-free concrete. The results are reasonably comparable. The difference in the initial $E_{corr}$ (-0.578 V and -0.460 V in the two cases) is attributed to the system being allowed a longer time to equilibrate in this experiment than in the original one. The $E_{corr}$ variation in both cases with inhibitor injection is compared with that in the case of $Ca^{2+}$ ion injection without inhibitor in Figure 5-6. Clearly, the electrical injection of inhibitor is effective in increasing the $E_{corr}$ of rebar steel to the recommended protection levels.

We performed another set of experiments using smaller amounts of $TEPNO_2$ (50 mM and 35 mM instead of the commonly used 100 mM solution) in the top compartment. However, to 25 mL of this solution we also added 20 mg of sodium glycinate, 15 mg of hydrazine hydrate, and $Ca(OH)_2$ until the solution was saturated. Sodium glycinate and hydrazine hydrate were added to the mixture because a previous U.S. Patent (4,365,999) described the addition of these two chemicals to sodium nitrite in formulating a corrosion inhibitor for steel in mortar or concrete. The objective was to determine whether less $TEPNO_2$ could be used in the presence of the two additives. Thus, in this case we used a completely novel inhibitor formulation containing the cationic inhibitor $TEPNO_2$. Electrical fields of 7.5 V/cm for the 50 mM $TEPNO_2$ solution and 7 V/cm for the 35 mM $TEPNO_2$ solution were applied. Corrosion potentials were monitored while the inhibitor was being injected, and the $R_p$ values were measured at the end of the experiment using AC impedance spectroscopy. Figure 5-7 shows the variation in $E_{corr}$ over the duration of inhibitor injection with this new inhibitor formulation.

AC impedance spectra at the end of the experiments showed two relaxations, a larger one appearing at higher frequencies and a smaller one at lower frequencies. We believe that the larger relaxation is due to a coating on the surface and the smaller to the interfacial process representative of the corrosion reaction. The coating resistivities were 16,726 and 20,650 $\Omega$ cm$^2$ and the $R_p$ values 3972 and 5893 $\Omega$ cm$^2$ with $TEPNO_2$ concentrations of 35 and 50 mM, respectively. If these $R_p$ values are compared with the 865 $\Omega$ cm$^2$ obtained for the inhibitor-free case, it is clear that the corrosion rates in the two cases have been lowered by 78% and 85%, respectively.

## Injection of Corrosion Inhibitors into Concrete Blocks

Studies of inhibitor injection into concrete blocks were performed using the arrangement shown in Figure 4-1. We performed these studies with inhibitor formulations of both $TEPNO_2$ and $TEPNO_2$ combined with sodium glycinate and hydrazine hydrate, with which we already had reasonably good success. A steel rebar embedded in a chloride-containing concrete block without the inhibitor showed an $E_{corr}$ of -0.421 V with respect to the Ag/AgCl, 0.1 N KCl reference electrode. The potentials were measured with respect to a saturated calomel reference electrode and converted to the Ag/AgCl, 0.1 N KCl scale to make comparisons with earlier results easier. The concrete blocks used in these studies measured 18 x 3 x 2 in. The steel rebar was embedded lengthwise 2 inches below the top surface.

When inhibitor injection was required, the inhibitor solution was placed on the top surface of a dry concrete block until it was absorbed, followed by a solution of calcium hydroxide. A calcium hydroxide-soaked sponge was placed on this surface with a DSA anode on top of it. An electrical field of 8 V/cm was applied to inject the cationic inhibitor into the chloride-contaminated concrete block. Figure 5-8 shows the variation in corrosion potentials of both the steel rebar and the rebar sample over the period of inhibitor injection. Clearly, in both cases the largest positive shift in $E_{corr}$ was observed after approximately 6-1/2 days of inhibitor injection. After this period of time,

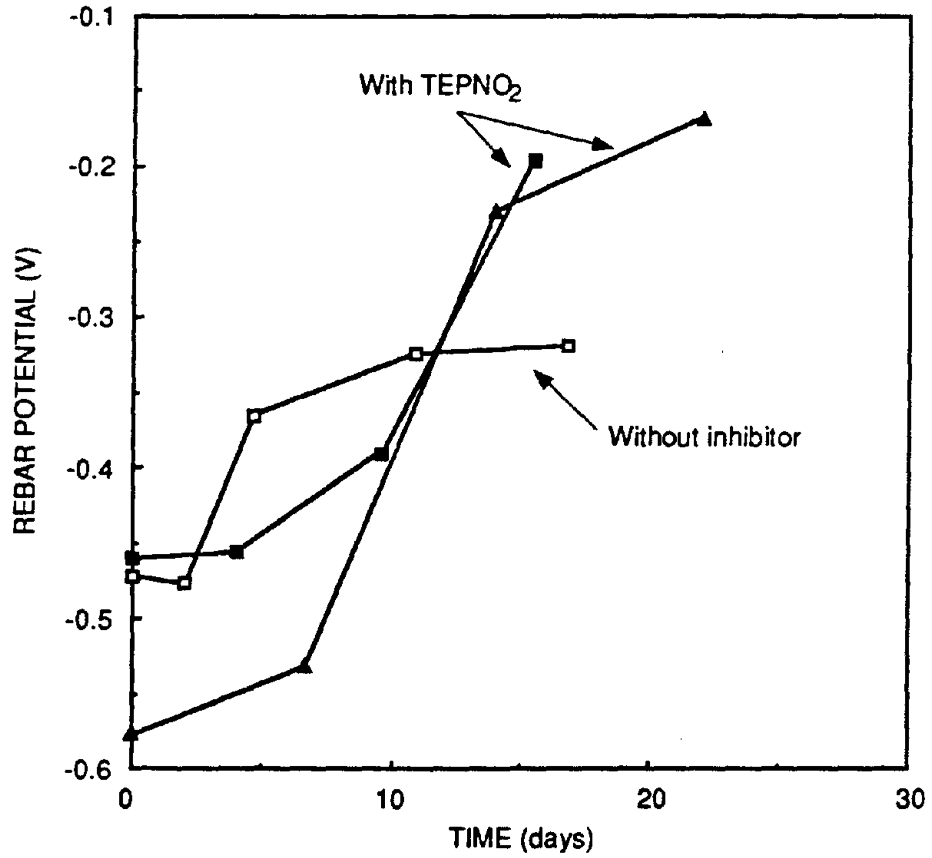

Figure 5-6. Rebar corrosion potential variation with time with and without TEPNO$_2$ injection. Applied field = 5V/cm.

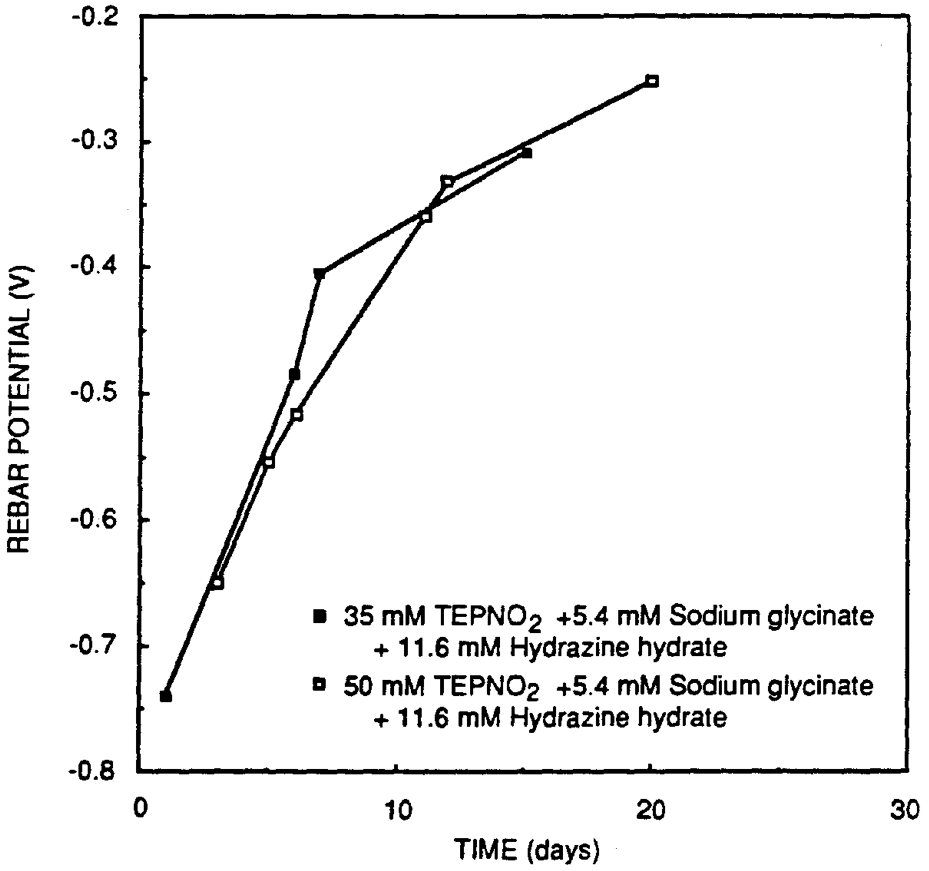

Figure 5-7. Rebar corrosion potential variation with time in the presence of inhibitor injections. Applied field = 7.5 V/cm.

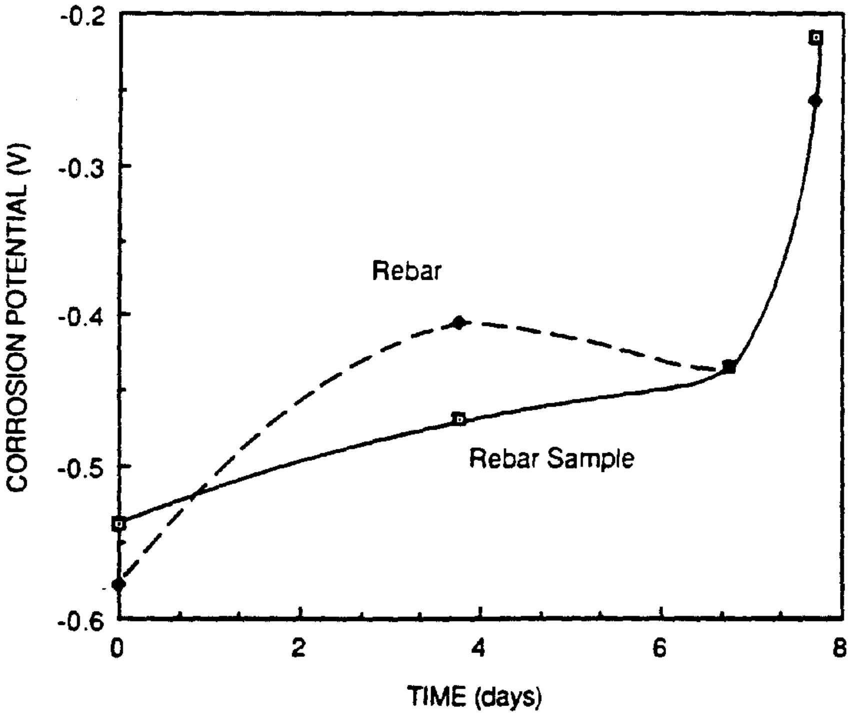

Figure 5-8. Rebar and rebar sample corrosion potential variation with inhibitor injection time. Applied field = 8V/cm 50 mM $TEPNO_2$ + 5.4 mM sodium glycinate + 15.5 mM hydrazine hydrate.

the $E_{corr}$ reached protection levels rapidly. This result clearly shows that inhibitor injection into concrete blocks is feasible and that adequate corrosion protection of corroding steel rebars can be achieved by using this technique.

# 6

# Accomplishments and Conclusions

We synthesized and identified four potential synergistic corrosion inhibitor candidates suitable for electrical injection into concrete for steel rebar corrosion protection: tetramethylphosphonium nitrite, tetraethylphosphonium nitrite, tetrabutylphosphonium nitrite, and tetraphenylphosphonium nitrite, all of which showed inhibitor efficiencies in the range 63-85%.

We also conducted electromigration studies of inhibitor ions through cement and concrete disks. We showed that cationic inhibitors such as $TEP^+$ and $TBP^+$ can be electrically injected into mortar and concrete matrices. We proved the feasibility of inhibitor injection by demonstrating the presence of inhibitor in the originally inhibitor-free cell compartment after application of the electrical field. This finding was further confirmed by the presence of inhibitor ions in the matrix after electromigration tests. We showed that an initial inhibitor concentration of 10 mM is not enough for electrical injection; with a concentration of 100 mM, inhibitor injection was observed within the first 50-100 hours. Thus, in our studies, we have proved the feasibility of inhibitor injection into concrete matrices by an electrical field-assisted approach.

Ion-chromatography was chosen for qualitative and quantitative analysis of ionic species present in anolytes, catholytes, and mortar and concrete matrix extraction solutions. This powerful technique provided analysis of all anions and cations in only two runs. The transport numbers of inhibitor cations $TBP^+$ and $TEP^+$ were calculated from the electromigrated cation content and the total charge passed during inhibitor injection. From the transport number data and the inhibitor injection data, the best inhibitor among those studied appeared to be $TEPNO_2$.

We demonstrated that electrical injection of corrosion inhibitors into chloride-contaminated mortar and concrete is feasible as well as practical. We showed that the $E_{corr}$ of a steel rebar embedded in $Cl^-$ containing concrete can be increased in the positive direction from -0.460 V to -0.196 V (vs. Ag/AgCl, 0.1 N KCl) by electrical injection of inhibitors. This value is reasonably close to the -0.104 V observed for a steel rebar in a chloride-free concrete environment. Thus, we achieved corrosion inhibition of steel rebar by nondestructive electrical injection of corrosion inhibitors into concrete.

We showed that $TEPNO_2$ is as good as a complex inhibitor formulation consisting of a solution of 7.25 mM $NaNO_2$, 0.53 mM sodium glycinate, and 1.93 mM hydrazine hydrate that has been recommended for mixing into concrete. We also showed that even reduced amounts of $TEPNO_2$, from 100 mM to 35 mM, are effective in corrosion inhibition. We demonstrated the beneficial effect of mixing $TEPNO_2$ with sodium glycinate and hydrazine hydrate to make a novel corrosion inhibitor formulation for electrical injection into concrete.

We repeatedly demonstrated the shift in the steel rebar $E_{corr}$ from more negative to more positive values during inhibitor injection. The fact that rebar potentials reach protection levels was further demonstrated by the enhanced $R_p$ values obtained after inhibitor injection.

Finally, we demonstrated the feasibility of inhibitor injection into chloride-contaminated concrete blocks. We also showed that such inhibitor injection can provide adequate corrosion protection of corroding steel rebars, as evidenced by a positive shift in the $E_{corr}$ to recommended protection levels. The major accomplishments we have achieved for SHRP in this project can be summarized as follows:

- Developed a novel electrically injectable inhibitor formulation for corrosion protection of steel rebars.

- Developed a new technique for electrically injecting corrosion inhibitors into chloride-contaminated concrete bridge components.

- Demonstrated that corroding steel rebars embedded in chloride contaminated-concrete blocks can be protected up to 78-85% with the current inhibitor by the electrical injection technique.

An important advantage of this technique is that the equipment required is similar to that used in cathodic protection and hence is familiar to highway bridge engineers. However, unlike cathodic protection, which requires a permanent installation, protection using inhibitor injection requires only a temporary installation for a few days.

Based on the experimental results, the following conclusions can be made on the electrical injection of corrosion inhibitors.

- Effective inhibitor injection occurs at an electrical field of 5 to 10 V/cm at a current density of 0.46 to 1.24 $mA/cm^2$ (0.4 - 1.1 A/sq. ft.) within a period of 10-15 days.

- At current densities of 0.50, 1.00 and 2-3 $mA/cm^2$ the inhibitor injection rate increased in the order 35, 95 and 420 $\mu g/cm^2/hr$ respectively for $TEPNO_2$. Thus, a doubling of the current density provides an approximately 3 to 4 times increase in the inhibitor injection rate. In a practical sense a current density of approximately of 1 $mA/cm^2$ appears desirable.

- An inhibitor injection current density of 1 $mA/cm^2$ (900 $mA/ft^2$) is 900 times higher than that required for cathodic protection (i.e. 1 $mA/ft^2$). Thus, under rebar cathodic control, the inhibitor injection rate could be more than 1000 times slower, requiring longer times to achieve the desired corrosion protection.

- After inhibitor injection, the rebar potential continues to shift in the positive direction over the tested period of 3 to 4 weeks indicating that chloride remigration, if it does occur, is not effective in increasing the rebar corrosion rate. However, a long term study (> 12 months) with sodium chloride ponding is necessary before a decision is made on the effectiveness of the inhibitor injection against chloride remigration.

# 7

# Recommendations

During the course of this project we demonstrated that electrical injection of inhibitors can provide up to 78-85% corrosion protection of rebar steel. We believe this level of protection can be increased to 90-100% with improvements in corrosion inhibitor formulation and optimization of the application technology. We recommend that the following research be pursued before the application of this technology in field studies and to actual bridge decks.

- The inhibitor primarily used in this study has an efficiency of 78%. We believe this efficiency should be increased above 90% so that more than 85% protection of steel rebars can be achieved. Thus, we strongly recommend the development of inhibitors that can provide efficiencies in the range 90-100%.

- Once corrosion protection is achieved by inhibitor injection, we do not know how long the protection lasts. Thus, it is necessary to perform a long-term study (one to two years) to determine the degree of retention of the inhibitor so that we can obtain information on the required frequency of inhibitor application.

- Once the inhibitor injection has been completed, it is important to know how effective the inhibitor will be against chloride remigration. We believe a study is required to address this question, particularly from the viewpoint of its long-term operation. Thus, we propose a study to monitor the corrosion of steel rebars after inhibitor injection over a period of six months to one year with and without intermittent salt spray.

- A study comparing steel rebar corrosion following inhibitor injection against situations involving cathodic protection should be performed. It must be emphasized that cathodic protection requires a permanent installation, whereas inhibitor injection and subsequent corrosion protection requires only a few days temporary installation.
- From a practical viewpoint, we believe a study involving a precorroded steel rebar embedded in chloride-contaminated concrete would be extremely useful. Such a study would provide information on the degree of protection afforded by inhibitor injection in a deteriorating situation.

From the experience gained during this study, we recommend that the proposed optimization studies be performed on concrete blocks measuring 18 x 4 x 4 in; final studies should be performed with concrete blocks measuring 2 ft. x 2 ft. x 8 in. The concrete block, in the former case, should have a single steel rebar along the 18-in. dimension, and the block in the latter case should have a typical bridge deck type of rebar network laid in the 2 x 2 ft. plane.

# References

1. Stern, M. and A. L. Geary. 1957 J. Electrochem. Soc. 104:56.
2. Epelboin, I., P. Morel, and H. Takenouti. 1971. J. Electrochem. Soc. 118: 1282.
3. Epelboin, I., M. Keddam, and H. Takenouti. Third European Symposium on Corrosion Inhibitors, Ferrara, Italy 1970, p. 237.